J. Fluid Mech. (1997), *vol.* 333, *pp.* 375–402

The instability of the shear layer separating from a bluff body

By ANIL PRASAD AND CHARLES H. K. WILLIAMSON
Mechanical and Aerospace Engineering, Cornell University, Ithaca, NY 14853, USA

(Received 17 April 1996 and in revised form 16 September 1996)

Notwithstanding the fact that the instability of the separated shear layer in the cylinder wake has been extensively studied, there remains some uncertainty regarding not only the critical Reynolds number at which the instability manifests itself, but also the variation of its characteristic frequency with Reynolds number (Re). A large disparity exists in the literature in the precise value of the critical Reynolds number, with quoted values ranging from $Re = 350$ to $Re = 3000$. In the present paper, we demonstrate that the spanwise end conditions which control the primary mode of vortex shedding significantly affect the shear-layer instability. For parallel shedding conditions, shear-layer instability manifests itself at $Re \approx 1200$, whereas for oblique shedding conditions it is inhibited until a significantly higher $Re \approx 2600$, implying that even in the absence of a variation in free-stream turbulence level, the oblique angle of primary vortex shedding influences the onset of shear-layer instability, and contributes to the large disparity in quoted values of the critical Reynolds number. We confirm the existence of intermittency in shear-layer fluctuations and show that it is not related to the transverse motion of the shear layers past a fixed probe, as suggested previously. Such fluctuations are due to an intermittent streamwise movement of the transition point, or the location at which fluctuations develop rapidly in the shear layer.

Following the original suggestion of Bloor (1964), it has generally been assumed in previous studies that the shear-layer frequency (normalized by the primary vortex shedding frequency) scales with $Re^{1/2}$, although a careful examination of the actual data points from these studies does not support such a variation. We have re-analysed all of the actual data points from previous investigations and include our own measurements, to find that none of these studies yields a relationship which is close to $Re^{1/2}$. A least-squares analysis which includes all of the previously available data produces a variation of the form $Re^{0.67}$. Based on simple physical arguments that account for the variation of the characteristic velocity and length scales of the shear layer, we predict a variation for the normalized shear-layer frequency of the form $Re^{0.7}$, which is in good agreement with the experimental measurements.

1. Introduction

The separated shear layer is one of the three fundamental ingredients which constitutes the flow past a bluff body, the other two being the wake and the boundary layer. The focus of the present study is the instability of the shear layer separating from the sides of a circular cylinder. Although a number of investigations have addressed this instability, there remains some uncertainty regarding the critical Reynolds number

at which the instability first manifests itself, and the variation of its characteristic frequency with Reynolds number, both of which have a surprising scatter in the literature.

The separating shear layer from a cylinder becomes unstable for Reynolds numbers (Re) of the order of 1000. The primary wake instability, which commences at the much lower Reynolds number of about 49, results in the classical von Kármán vortex street configuration and develops three-dimensionalities for $Re > 190$ (see Williamson 1996*a* for a comprehensive review). The primary wake instability, now known to be the result of a Hopf bifurcation, scales with the cylinder diameter. On the other hand, the shear-layer instability which develops by the action of a Kelvin–Helmholtz mechanism, scales with the thickness of the separating shear layer, which is generally a small fraction of the cylinder diameter. Consequently, the length and time scales of the shear-layer instability are much smaller than those of the wake instability. The ensuing small-scale vortices which form within the separated shear layer, visually appear similar to those found in the plane mixing layer between co-flowing streams of unequal velocity. Nevertheless, some distinct differences are found due to the spatial restriction imposed by the formation of the large-scale Kármán vortices: in order to be visible, the shear-layer instability necessarily needs to develop and to then undergo significant amplification *before* the shear layer rolls up to form the primary Kármán vortex. These ideas were used by Roshko (1993) and Williamson (1996*a*) in a simple analysis to suggest a value for the Reynolds number below which shear-layer instability would not be perceived. However, by artificially suppressing primary vortex formation, further similarities emerge between the separated shear layer and plane mixing layers. Using a 'splitter plate' (Roshko 1954) to inhibit the roll-up of primary vortices, Unal & Rockwell (1988*b*) found that the shear-layer instability exhibits significant amplification at the $1/2$-subharmonic of the naturally occurring shear-layer frequency, and suggested that this is due to the coalescence of small-scale vortices, as is observed in other free shear layers. By moderating Kármán vortex formation with the use of permeable wake splitter plates, Cardell (1993) also observed the development of the $1/2$-subharmonic. In addition, he found that the separating shear layers exhibit self-similarity far downstream, as is observed in plane mixing layers. However, in the present study, we focus on the instability of the naturally evolving separated shear layer.

Over the past several decades, a number of investigations have addressed diverse aspects of shear-layer instability, some of which we highlight here. Linke (1931) and Schiller & Linke (1933) appear to be the first to have recognized that turbulence develops in the separated shear layers from a cylinder. They suggested, from their measurements of mean quantities, that the rapid increase in the base 'suction' coefficient (negative of base pressure coefficient) in the range $Re = 10^3$–10^5 is associated with the point of transition in the shear layers moving upstream as Re increases. However, it was not until much later that Bloor (1964) made the first systematic measurements of the characteristic frequency associated with the shear-layer instability. She labelled this the 'transition' frequency, in analogy with the instability observed in wall boundary layers. Subsequent investigators have used a variety of terminology including the 'Bloor–Gerrard' frequency, the 'Kelvin–Helmholtz' frequency and the 'secondary' frequency. However, we prefer to simply label it the shear-layer frequency (f_{SL}). Conventionally, f_{SL} is normalized by the Kármán vortex shedding frequency (f_K). Based on parameter variations similar to those of laminar boundary layers, Bloor (1964) suggested that f_{SL}/f_K should scale with $Re^{1/2}$. Since her pioneering work, other investigators including Smith, Moon & Kao (1972), Wei & Smith (1986),

Kourta *et al.* (1987) and Norberg (1987) have measured the shear-layer frequency. Many of these investigators attempted to fit their data to an $Re^{1/2}$-variation, although an examination of their actual data points does not support such a variation. Wei & Smith (1986) found that the normalized shear-layer frequency varies as $Re^{0.77}$ from hot-wire measurements and as $Re^{0.87}$ from flow visualization. They surmised that the former technique of measurement would inherently result in lower values of the shear-layer frequency, because the intermittent shear-layer fluctuations (induced by the transverse motion of the shear layer past a fixed probe), when transformed into the frequency domain produce spurious peaks in the spectrum. From his measurements, Norberg (1987) suggested that a single power law may not represent the variation of f_{SL}/f_K over the entire Re-range up to $Re = 10^5$ and found that a local maximum in the exponent occurs at $Re = 5000$. It therefore appears from the above discussion that the variation of the normalized shear-layer frequency with Re, remains an unresolved question.

A further pertinent question concerns the critical Reynolds number (Re_c) at which the shear-layer instability is first observed. It is evident from a survey of the literature that there exists a surprisingly large discrepancy in quoted values of Re_c, as the following examples illustrate: Gerrard (1978) suggested that $Re_c \approx 350$; Bloor (1964) detected the instability only for $Re > 1300$ from her hot-wire measurements; Unal & Rockwell (1988*a*) found, from their hot-film and flow visualization studies, that the instability could not be perceived for $Re < 1900$; more recently, Wu *et al.* (1996) have suggested that the critical Reynolds number can lie anywhere between $Re = 1000$ and $Re = 3000$, and that its precise value depends on background disturbance conditions. Although it is known that Re_c can depend on the level and spectral content of background disturbances (Unal & Rockwell 1988*a*), it appears that this large disparity may not be explained solely by this source, since much of the variation occurs under similar turbulence conditions. One may then suggest that three-dimensional near-wake phenomena would influence the development of the separated shear layer.

Three-dimensional wake phenomena such as parallel and oblique shedding can be controlled in the laminar shedding regime ($49 < Re < 190$) through the use of spanwise end manipulation (see review in Williamson 1996*a*). In a recent study, Prasad & Williamson (1995, 1997) have shown that the end boundary conditions can similarly be used to control parallel and oblique vortex shedding over long spanlengths, for $Re > 260$ and at least up to $Re \sim 10^4$, which is relevant to the present study. Several characteristic parameters measured in the wake display distinct differences between parallel and oblique shedding end conditions. One naturally questions whether the end conditions, which affect the primary vortex shedding, also affect the instability of the separated shear layer. This question, which was partially addressed in Prasad & Williamson (1996), forms the starting point of the present paper.

In § 3, the influence of end conditions on the instability of the shear layer is presented. We will show that the end conditions can significantly affect the critical Reynolds number for shear-layer instability. It also appears that shear-layer fluctuations display an intermittency, which we further characterize in § 4. Frequency measurements presented in § 5, show that a power law of the form $Re^{0.67}$ accurately represents the Re-variation of f_{SL}/f_K, when one considers data from all the investigators who have measured the shear-layer frequency. This is followed, in § 6, by an analysis, based on simple physical arguments, which suggests why one should naturally expect a power-law exponent larger than 0.5. We predict a Re-variation for the normalized shear-layer frequency, which compares well with the experimentally determined variation. Following this, we present a brief discussion and conclusions.

2. Experimental details

The experiments were performed in an open-circuit suction wind tunnel. The free-stream turbulence was less than 0.08% and flow uniformity better than 0.3% in the 12 in. × 12 in. test section, measured over the range of velocity from 0.5 to 14 m s^{-1}; the free-stream turbulence level was measured using an RMS meter with a frequency range of 10 Hz to 10 MHz. Cylinders of diameter 0.318, 0.635, 1.27 and 2.54 cm were mounted near the upstream end of the test section. The Reynolds number is defined as $Re = U_\infty D/\nu$, where U_∞ is the free-stream velocity and D is the cylinder diameter. Circular endplates (of diameter $= 10\,D$) were fitted on the cylinders to produce aspect ratios of 20–80; however, the cylinder of largest diameter, which was not fitted with endplates, delivered an aspect ratio of 12. The hot-wire measurements were performed on the cylinders of aspect ratio 40–80, with the cylinders of aspect ratio 12–20 being used solely for flow visualization. To produce parallel vortex shedding across the entire span, each endplate was positioned with its leading edge inclined inwards about 12°. By inclining each endplate in the same direction, oblique vortex shedding was induced. In the present paper, these endplate configurations are referred to as the parallel and oblique shedding conditions respectively.

The origin of the wake coordinate system is fixed on the axis of the cylinder. The x-axis is directed downstream, the y-axis is perpendicular (defined as transverse) to the flow direction and the cylinder axis, and the z-axis lies along the axis of the cylinder (defined as spanwise).

Wake velocity measurements were made, at the midspan of the cylinder, using a miniature hot-wire probe in conjunction with a two-channel anemometer system. Most of the single-point measurements were made near the outer edge of the shear layer, at $x/D = 1.0$, except where indicated. A Stanford Research Systems SR760 spectrum analyser was used for the spectral measurements. Long-time-averaged velocity spectra were produced by averaging measured spectra for time durations in excess of 10 000 vortex shedding cycles. Fluctuating RMS velocities at the vortex shedding frequency and the shear-layer frequency were calculated using amplitudes of the corresponding spectral peaks determined from long-time-averaged spectra. The total velocity fluctuation intensity was measured on a Hewlett–Packard 3400A true-RMS meter. Time traces were recorded on a computerized data-acquisition system with a sampling rate of 100 kHz.

Flow visualization was conducted using a vertical smoke-wire system, as originally described by Corke *et al.* (1977). A GenRad 1540 Strobolume provided the intense illumination required to capture photographic images on ISO 400/27° film with a Nikon F3 camera.

3. Influence of end conditions on the development of shear-layer fluctuations

We focus, in this section, on the effect of the spanwise end boundary conditions on the development of the separated shear layer. One may approximate reasonably well the mean velocity profile across the shear layer by the error function, as shown in figure 1 for parallel shedding conditions. The error function profile is selected in preference to the more frequently used hyperbolic-tangent profile because δ_ω/θ (δ_ω = shear-layer vorticity thickness, θ = shear-layer momentum thickness) for the former matches better the experimentally determined value, an observation also made by Cardell (1993). We shall use the mean profile later to estimate the extent of

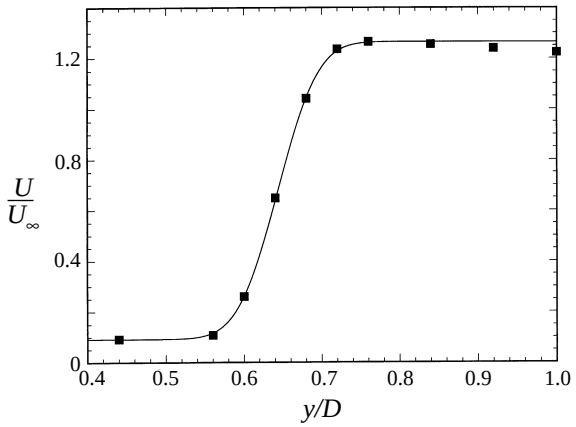

FIGURE 1. Mean velocity distribution across the shear layer at $Re = 2000$. The data for parallel shedding at $x/D = 1.0$ are presented for the cylinder of diameter 0.318 cm. The error function, shown by the solid line, approximates the profile accurately.

transverse motion (sometimes referred to as 'flapping') of the shear layer. The error function profile approximates the mean velocity for oblique shedding conditions as well, implying that the gross features of the flow, in this vicinity, are not altered by the primary vortex shedding angle. However, distinct differences between parallel and oblique shedding are clearly observed in measurements of velocity fluctuation within the shear layer. Long-time-averaged velocity spectra are shown in figure 2, for both parallel and oblique shedding conditions, at $Re = 1000$ and $Re = 1200$. Both the spectra obtained at $Re = 1000$ appear similar, with prominent peaks only at f_K and $2f_K$. However, at $Re = 1200$, for parallel shedding conditions, an additional peak appears at a frequency f_{SL} ; in contrast, no such peak appears for oblique shedding conditions at the same Reynolds number. A peak at f_{SL} was defined to exist if the level of energy at the peak exceeded the noise level at surrounding frequencies. It appears that the critical Reynolds number to observe shear-layer instability is lower in the case of parallel shedding.

Differences between parallel and oblique shedding are found to persist as Re increases. Spectra at $Re = 2700$, shown in figure 3, indicate that for parallel shedding conditions in (a) the spectral peak at f_{SL} is very well-defined, whereas for oblique shedding conditions in (b) the peak is barely visible. The spectral peak at f_{SL} appears to be relatively broad compared to the distinctly sharp peak at f_K, as seen clearly in figure 3(a). The sharp peak at f_K is indicative of the existence of an absolutely unstable process which is responsible for the relatively coherent and energetic velocity fluctuations associated with Kármán vortex formation. In contrast, the broad-band peak at f_{SL} is consistent with the convectively unstable nature of shear-layer instability. Evidence of such a broad-band peak at f_{SL} is also found in the theses of Norberg (1987) and Cardell (1993). Based on analogies with plane mixing layers, Cardell (1993) suggested that one should naturally expect a broad peak at f_{SL}, because of the unsteady environment in which the shear-layer instability develops. The most unstable frequency, f_{SL}, scales with the velocity outside the separation point and with the momentum thickness of the shear layer. Temporal variations in the velocity scale arise due to the presence of large-scale Kármán vortex formation. Furthermore, due to the slight oscillation of the point of separation (also caused by Kármán vortex formation), one can expect some variability in the value of the

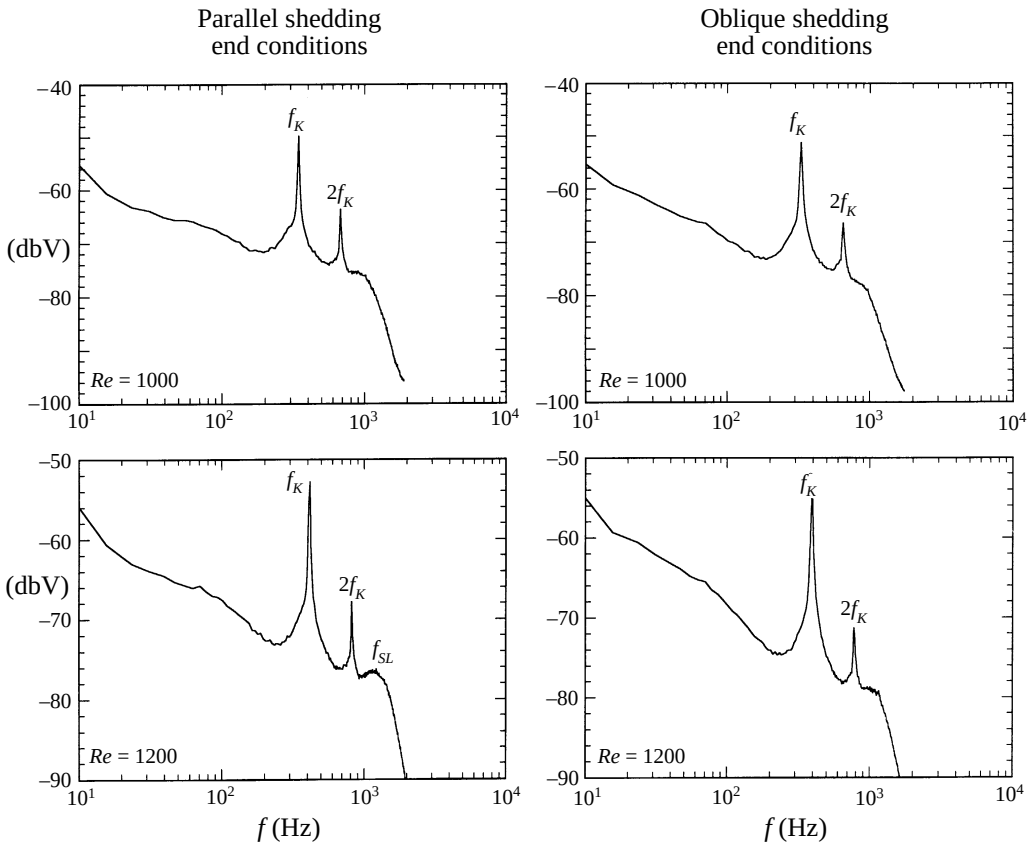

FIGURE 2. Influence of end conditions on velocity spectra in the shear layer. The spectra at $Re = 1000$, for parallel and oblique shedding conditions appear similar. However, at $Re = 1200$, the spectrum for parallel shedding displays a broad peak at f_{SL}, whereas no such peak is observed for oblique shedding at this Re. The prominent spectral peaks indicated are the Kármán shedding frequency, f_K, its first harmonic, $2f_K$, and the shear-layer frequency, f_{SL}. The measurements are made at $x/D = 1.0$ and $y/D \approx 0.8$.

momentum thickness as well. Both of these factors would contribute to a variation (in time) of the most unstable frequency, and to the broad-band peak at f_{SL}, in velocity spectra.

Returning to figures 2 and 3, we observe that the peak at f_{SL} is larger in magnitude at $Re = 2700$ than it is at $Re = 1200$. This can be conveniently quantified as the turbulence intensity at the shear-layer frequency, $(u'_{rms}/U_\infty)_{f_{SL}}$, which is found to increase with Re as one might expect, and shown in figure 4. Peterka & Richardson (1969) also observed, from limited measurements, that the amplitude of fluctuation at the shear-layer frequency increases in magnitude as Re increases. However, we find that the increase for parallel shedding is markedly larger than it is for oblique shedding, suggesting that the instability is, in some fashion, moderated by the oblique shedding conditions. The data in figure 4 also permit us to determine the critical Reynolds number for shear-layer instability, by extrapolating the curves to the noise level in the spectrum when the peak at the shear-layer frequency disappears. It is necessary to mention here that unlike the case of primary wake instability for which a precise mathematical definition of critical Reynolds number exists, the present usage

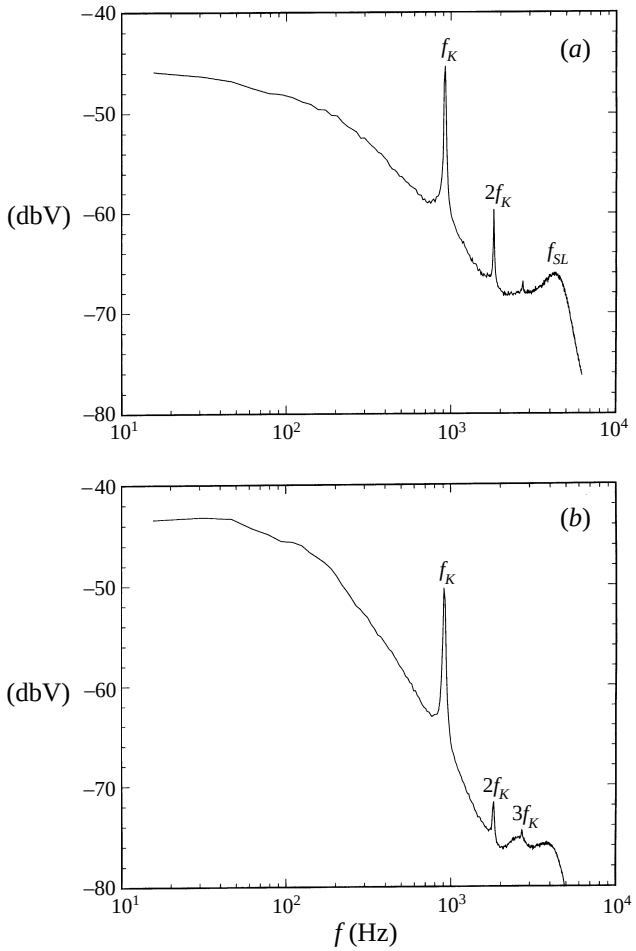

FIGURE 3. Comparison of spectra at $Re = 2700$. The peak at f_{SL} is very well-defined in the case of parallel shedding (*a*), whereas it is barely visible for oblique shedding in (*b*). The measurements are made at $x/D = 1.0$ and $y/D \approx 0.8$.

of the term for the case of shear-layer instability refers to the Reynolds number below which a peak at the shear-layer frequency could not be measured in velocity spectra. We find, for parallel shedding conditions, $Re_c \approx 1200$, whereas for oblique shedding conditions a considerably larger value of $Re_c \approx 2600$ is found. It is well-known that the level of free-stream turbulence can affect the value of the critical Reynolds number (Unal & Rockwell 1988*a*). However, in the absence of a variation in the free-stream turbulence level, we find that the critical Reynolds number can be significantly affected by the end conditions on the cylinder, and indeed by the angle at which the primary vortices are shed.

Since our wake measurements were made exclusively at midspan, there still remains an important question regarding the spanwise structure of the shear-layer instability. In particular, we ask whether the shear-layer instability waves are always parallel to the axis of the cylinder, or if indeed they adopt the spanwise structure of the Kármán vortices. Smoke-wire flow visualization, presented in figure 5, demonstrates that the shear-layer instability is very nearly parallel to the cylinder axis, irrespective

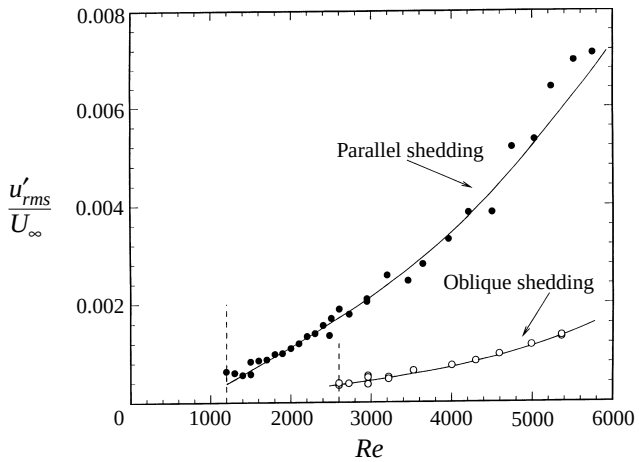

FIGURE 4. Variation of the intensity at the shear-layer frequency, $(u'_{rms}/U_\infty)_{f_{SL}}$, with Re. The intensity which increases rapidly for parallel shedding conditions, however, increases only moderately for oblique shedding conditions. It is possible to deduce that the instability sets in at $Re \approx 1200$ with parallel shedding but is inhibited by oblique shedding till $Re \approx 2600$, as indicated. The measurements are made at $x/D = 1.0$ and $y/D \approx 0.8$.

of whether the primary vortex shedding is parallel, shown in (*a*), or oblique as shown in (*b*). We find that the instability of the separated shear layer is on the whole two-dimensional along the span, in agreement with the suggestion of Braza, Chassaing & Ha Minh (1990). It, therefore, appears that the most unstable mode in the shear layer is two-dimensional, despite the fact that the base flow in the parallel shedding case is different from the oblique shedding case, as we explain presently.

One naturally questions why the shear-layer instability is inhibited until $Re_c \approx 2600$, for oblique shedding conditions. One suggestion may be made based on the sensitivity of the separated shear layer to perturbations that occur near the separation point. These perturbations, which are induced by primary vortex formation further downstream, act on the shear layer by an 'upstream influence', a suggestion made by Unal & Rockwell (1988*a*). Our measurements indicate that primary vortex shedding is less energetic for oblique shedding than it is for parallel shedding, throughout the velocity spectrum, and especially in the band of receptivity of the shear-layer instability. The separated shear layer acts essentially as a selective amplifier of perturbations. If the fluctuations induced by the upstream influence of primary shedding are considered as its 'input', then it is clear that the amplitude of the shear-layer instability measured at a fixed location will be higher in the parallel shedding case, and hence will be elevated above the noise level at lower Re, than in the oblique shedding case.

The upstream influence mentioned above, however, is not the sole contributor to the difference observed in shear-layer fluctuations between parallel and oblique shedding conditions. The perturbations that act on the region near the separation point would act on different base flows in the two cases. For parallel shedding, since vortex formation occurs in-phase along the span, the velocity at the separation point is spanwise correlated, and the separated shear layer develops in a manner similar to a two-dimensional mixing layer. However, in the case of oblique shedding since the velocity at separation is not spanwise correlated, the separated shear layer can no longer be described as two-dimensional. One can imagine that the growth rate of

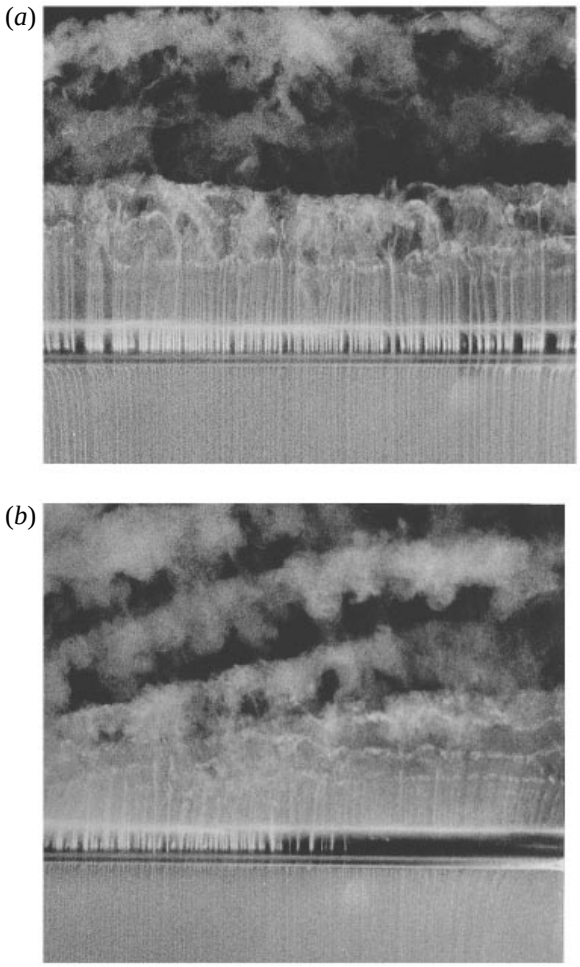

FIGURE 5. Spanwise flow visualization of the shear-layer instability for (*a*) parallel shedding end conditions at $Re = 4000$ and (*b*) oblique shedding end conditions at $Re = 5800$. It appears that the shear-layer instability is on the whole spanwise two-dimensional, irrespective of the particular end boundary conditions on the cylinder. The smoke wire, which is parallel to the cylinder of diameter 1.27 cm, is positioned directly upstream of its front stagnation point, and the flow direction is upwards.

disturbances in this three-dimensional shear layer is diminished in comparison to its two-dimensional counterpart.

Another point which we will address in more detail in the following section concerns our observation that the instability actually manifests itself only intermittently, despite the fact that long-time-averaged velocity spectra show a distinct peak at the shear-layer frequency. Such intermittency has been observed before, since some experimental evidence of its presence can be found in the theses of Norberg (1987) and Cardell (1993). The upper time trace in figure 6(*a*) clearly demonstrates this intermittency; the 'packets' of high-frequency fluctuations correspond to the shear-layer instability. For oblique shedding, no such intermittent fluctuations are observed at this particular *Re*. Furthermore, the time traces demonstrate that when the shear-layer instability does manifest itself in the parallel shedding case, its amplitude of fluctuation is much

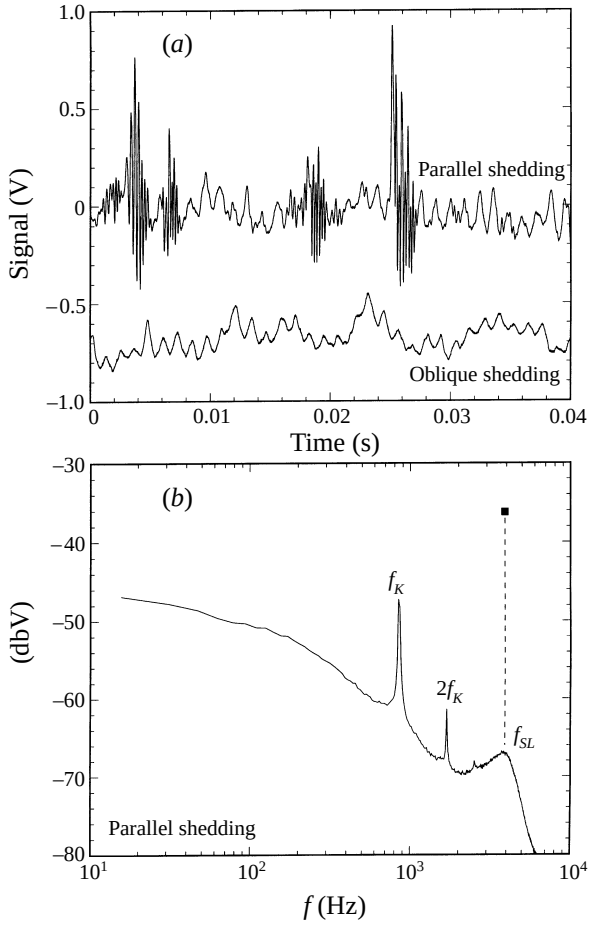

FIGURE 6. Velocity fluctuations within the shear layer at $Re = 2500$. In (a), we show time traces with parallel and oblique shedding end conditions. 'Packets' of shear-layer fluctuations are observed for parallel shedding, but not for oblique shedding at this Re. In (b), the solid square symbol represents an estimate of the level of shear-layer fluctuations from the time trace in (a) had they occurred continuously instead of intermittently. The measurements are made at $x/D = 1.0$ and $y/D \approx 0.8$.

larger than fluctuations at the primary shedding frequency. This is, however, not apparent from the long-time-averaged velocity spectra of figure 3(a). In order to clarify this point, we have computed (from the trace in figure 6a) the level of shear-layer fluctuations had they occurred continuously instead of intermittently, and this is shown as the solid square symbol on the spectrum in figure 6(b). It is found to be several times larger than the peak at f_K, at the location of hot-wire measurement. Therefore, the broad-band peak at f_{SL} appears diminished in long-time-averaged velocity spectra, because the shear-layer instability is intermittently manifested.

The inception of instability in the shear layers would naturally be expected to have an impact on characteristic near-wake parameters. It is observed from figure 7(a) that the fluctuation intensity at the shedding frequency, $(u'_{rms}/U_\infty)_{f_K}$, measured in the shear layer at $x/D = 1.0$, develops an upward trend for $Re > 1200$ with parallel shedding, but not with oblique shedding in this range of Reynolds number. These trends are consistent with similar variations in $(u'_{rms}/U_\infty)_{f_K}$ measured further downstream at $x/D = 10$ by Prasad & Williamson (1995, 1997). Interestingly, the

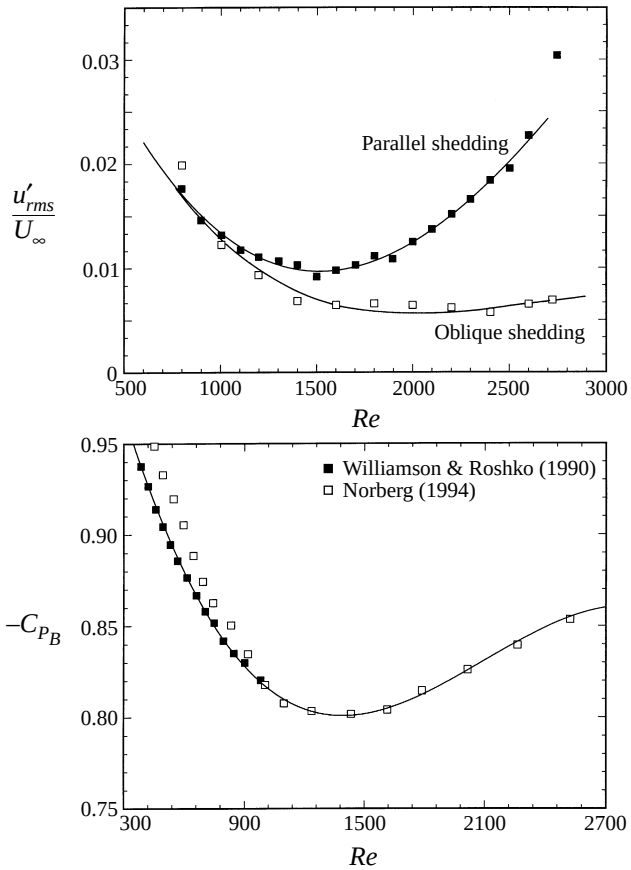

FIGURE 7. Characteristic parameters in the near wake. In (*a*), the variation of $(u'_{rms}/U_\infty)_{f_K}$ for parallel shedding develops an upward trend for $Re > 1200$, although not so for oblique shedding. The measurements are made at $x/D = 1.0$ and $y/D \approx 0.8$. In (*b*), measurements show that the base suction coefficient also demonstrates a broad minimum at $Re \approx 1200$. The data from Norberg (1994) were measured under conditions which effectively promoted parallel shedding.

careful measurements of Norberg (1994) demonstrate that the coefficient of base suction also develops an upward trend for $Re > 1200$, included here in figure 7(*b*). The base suction coefficient is defined by

$$-C_{P_B} = -\frac{p_B - p_\infty}{\frac{1}{2}\rho U_\infty^2},$$

where p_B is the pressure at the base of the cylinder and p_∞ is the static pressure in the free stream. His $(-C_{P_B})$ measurements were made under conditions which inadvertently promoted parallel shedding, therefore producing the observed variation. These upward trends occur because the development of instability in the shear layers creates an increase in the cross-sectional $(-\overline{u'v'})$ Reynolds stress, which is balanced in the mean recirculation region of the wake by an increase in the coefficient of base suction.

It appears from the above discussion that the main effect of oblique shedding conditions is to moderate the shear-layer instability, thereby producing a higher critical Reynolds number in comparison with parallel shedding conditions. In what

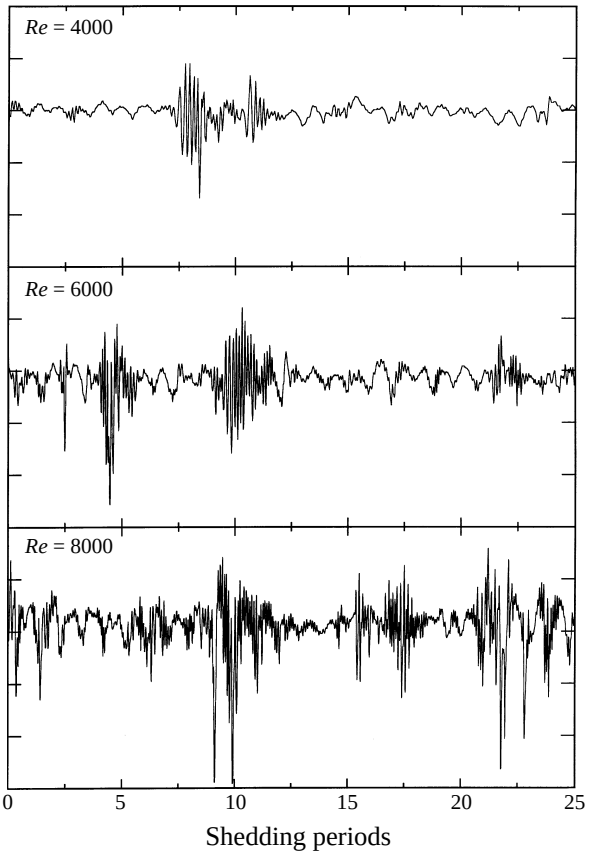

FIGURE 8. Time traces show that as Re increases, the packets of fluctuation corresponding to the shear-layer instability become more frequent. The measurements are made at a fixed point in the shear layer near its outer edge, at $x/D = 1.0$.

follows, our attention will be directed only to the case of parallel shedding end conditions.

4. Intermittency of shear-layer fluctuations

We would now like to focus our attention on the intermittency of shear-layer fluctuations, with the aim of understanding the cause for this intermittency, using measurements which characterize its variation with Reynolds number, and with streamwise distance. With increasing Re, we find that the packets of shear-layer fluctuation occur more frequently, as shown in figure 8. The measurements are made with the hot-wire probe fixed at a location near the outer edge of the shear layer. It is also evident, from figure 8, that the maximum amplitude of the shear-layer fluctuations increases with Re, which is in agreement with measurements presented in figure 4. In order to quantify the variation observed in figure 8, we define an intermittency factor (γ) as that fraction of total time when the high-frequency oscillations are present. Figure 9 shows that γ increases rapidly towards unity as Re increases; to obtain an unprejudiced estimate of γ, its value at each Re has been calculated from time traces spanning 25 primary shedding cycles. The calculated value of γ includes all of the high-frequency fluctuations observed, regardless of their amplitude of oscillation.

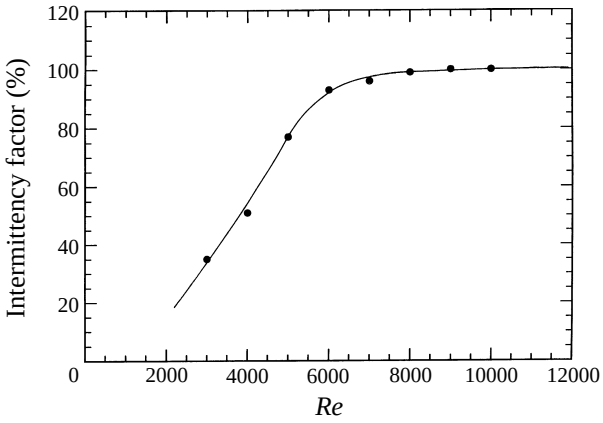

FIGURE 9. Variation of the intermittency factor γ with Re. We find that γ increases rapidly towards unity, as the Reynolds number increases. At each Re, the value of γ is calculated from time traces spanning 25 shedding cycles. The time traces are measured at a fixed point in the shear layer near its outer edge, at $x/D = 1.0$.

The increase, with Re, of the intermittency factor measured at a fixed point in the shear layer may in part be the effect of the region of instability moving upstream with increasing Re. This suggestion is based on the work of Linke (1931) and Schiller & Linke (1933), who determined that as Re increases, the point of transition in the shear layers advances upstream. This corresponds with an upstream motion of the location at which shear-layer fluctuations grow to perceptible proportions (see transition point as defined by Sato 1956 in §6), which can cause a fixed probe to detect more frequent shear-layer fluctuations, with increasing Re. To isolate the streamwise development of the shear-layer instability, we have recorded time traces at a fixed $Re = 4000$, for various downstream distances, as shown in figure 10. We find that packets of shear-layer fluctuation become more frequent as one travels downstream. Since the shear layer curves inwards as it travels downstream, the position of the probe was adjusted at each streamwise location, so as to lie near its outer edge. The intermittent fluctuations are observed to grow in magnitude with downstream distance, which is characteristic of convectively unstable flows, such as a plane mixing layer.

Having characterized some aspects of the development of intermittency, we now suggest a heuristic explanation for its existence. Wei & Smith (1986) conjectured that the observed intermittency is due to the transverse motion of the shear layer. This would cause a stationary probe to sense, only periodically, fluctuations corresponding to the shear-layer instability. Recently, Cardell (1993) has indicated that it is unlikely that intermittency is caused by this transverse motion, because it would imply that the probe would record very low velocities (typical of the mean recirculation zone) and produce characteristic low-velocity spikes which would appear in every shedding cycle. However, such spikes are seldom observed, and when they do occur, are not found to appear consistently in every shedding cycle, suggesting that the reason for intermittency lies elsewhere. To establish that intermittency is not caused by the transverse motion, we have quantified the latter by using the upper time trace in figure 6(*a*). For our estimate, we assume that the vortex shedding oscillation observed in the time trace (at $x/D = 1.0$) is caused solely by the mean velocity profile of the shear layer moving past the fixed probe, at the primary shedding frequency. Such a calculation will over-estimate the transverse motion since, as one can imagine,

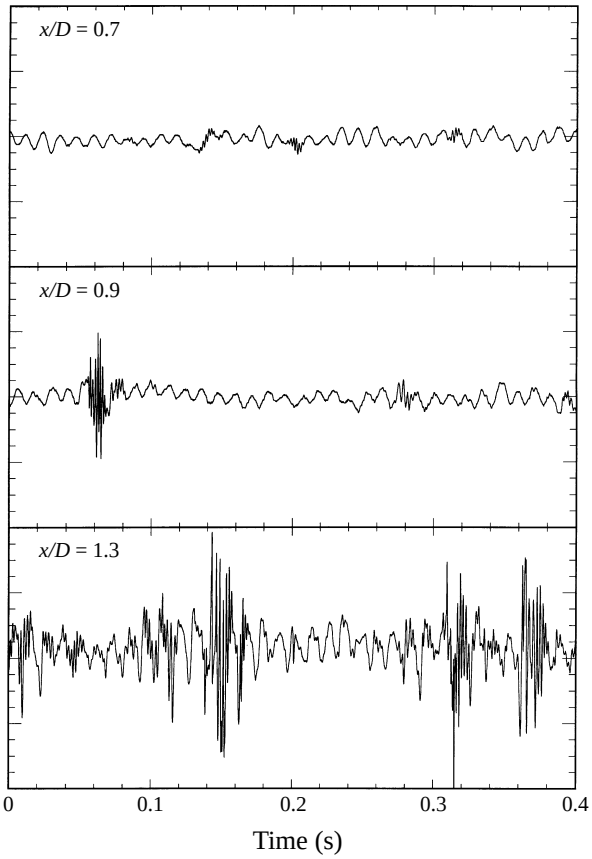

FIGURE 10. Time traces obtained at $Re = 4000$ show that the intermittency factor would increase with downstream distance. The hot-wire probe is positioned near the outer edge of the shear layer, at each streamwise location.

primary vortex formation would itself induce substantial fluctuating velocities in the shear layer. It appears surprising that even an over-estimate produces a transverse motion which is barely 8% of the thickness of the shear layer (defined to be the transverse distance over which the mean velocity varies from $0.01\Delta U$ to $0.99\Delta U$, where ΔU is the mean velocity difference across the shear layer). Therefore, one can conclude that even as far downstream as $x/D = 1.0$, the intermittency of shear-layer fluctuations is not caused by a transverse motion of the separated shear layers. A further deduction from this result is that the transverse motion cannot cause the observed intermittency in the measurements of Wei & Smith (1986), which were made at $x/D = 0.6$, since it is known that the transverse motion diminishes as one travels upstream in the shear layer.

Any plausible explanation for intermittency would have to account for the fact that it is present even when primary vortex formation is moderated or suppressed, as documented by Cardell (1993). This implies that phenomena associated with primary Kármán vortex shedding alone cannot completely explain intermittency. The knowledge that the intermittency factor increases with Re and downstream distance seems to suggest that the entire region of instability – from its inception to the location at which well-defined shear-layer vortices are formed – moves randomly upstream and downstream. In addition to the random motion described above, there is the distinct

possibility that the spontaneous generation of certain three-dimensional streamwise structures in the near wake, which have been referred to as Mode B by Williamson (1988), contribute significantly to the intermittency. These Mode B structures which have a typical spanwise wavelength of about one diameter are found to exist in the braid region between consecutive Kármán vortices (Williamson 1988, 1996*b*), for $Re > 260$ and at least up to $Re = 10^4$ (Lin, Vorobieff & Rockwell 1996). Temporal changes in the three-dimensional structure at $Re > 1000$ may disrupt the ordered formation of the predominantly two-dimensional shear-layer vortices and lead to the observed intermittency.

Flow visualization allows observation of the streamwise evolution of instability over the entire length of the shear layer. In figure 11, we present typical examples of the cross-sectional view of the near wake, indicating clearly the shear-layer vortices, with the smoke-wire placed immediately downstream of the base of the cylinder. It is of interest to note that flow visualization with the smoke-wire placed upstream of the cylinder produced almost no evidence of the shear-layer instability. To explain this apparent paradox, we note that in order to perceive shear-layer instability using smoke-wire visualization, smoke particles would need to be introduced either directly into the separated shear layer, as is done in figure 11, or into the cylinder wall boundary layer. With regard to the latter technique, since all streamlines that originate upstream of the cylinder always remain outside the boundary layer, it appears nearly impossible to introduce smoke into the cylinder wall boundary layer using an upstream-mounted smoke wire, which is consistent with our observation. The photographs in figure 11 demonstrate clearly that the instability intensifies as Re increases. In addition, a comparison between the images at $Re = 4000$ and $Re = 10\,000$ indicates that the region of clearly formed shear-layer waves or vortices advances upstream as Re is increased. Furthermore, from a collection of photographs at $Re = 5000$ (not shown), we find that at a fixed streamwise location, the instability is at some instants barely perceptible, while at other instants has evolved into discrete shear-layer vortices, providing visual evidence for the notion that the transition point moves intermittently upstream and downstream. We also note from figure 11 that the shear-layer instability appears to be in-phase across the wake, an observation also made by Gerrard (1978). However, although such in-phase behaviour was observed in the majority of our photographs, other configurations did manifest themselves. The in-phase behaviour is perhaps linked to the intermittency as we explain below. It is observed from the time traces, such as in figure 8, that the amplitude of the shear-layer fluctuations can be classified into those which are large compared to the primary vortex shedding oscillations and those which are small compared to these oscillations. Although the foregoing discussion on intermittency did not address this aspect, we would now like to suggest that it is the in-phase configuration which is responsible for the large-amplitude shear-layer fluctuations observed in the time traces. Since in the range of Reynolds numbers considered here Kármán vortex formation occurs somewhat downstream of the cylinder, one would expect a certain degree of feedback between the two separating shear layers, which arises due to their proximity. It is conceivable that this feedback between the shear layers enhances fluctuations in the shear layer to levels which are beyond those expected from the linear instability of a shear layer developing in isolation. Moreover, one could consider the possibility of mode competition in the system consisting of two shear layers separated spatially by a distance of one cylinder diameter. The instability of such a system would admit both a symmetric and an antisymmetric mode. If the most unstable frequency of each of these two modes is not too dissimilar, then the swapping between large-

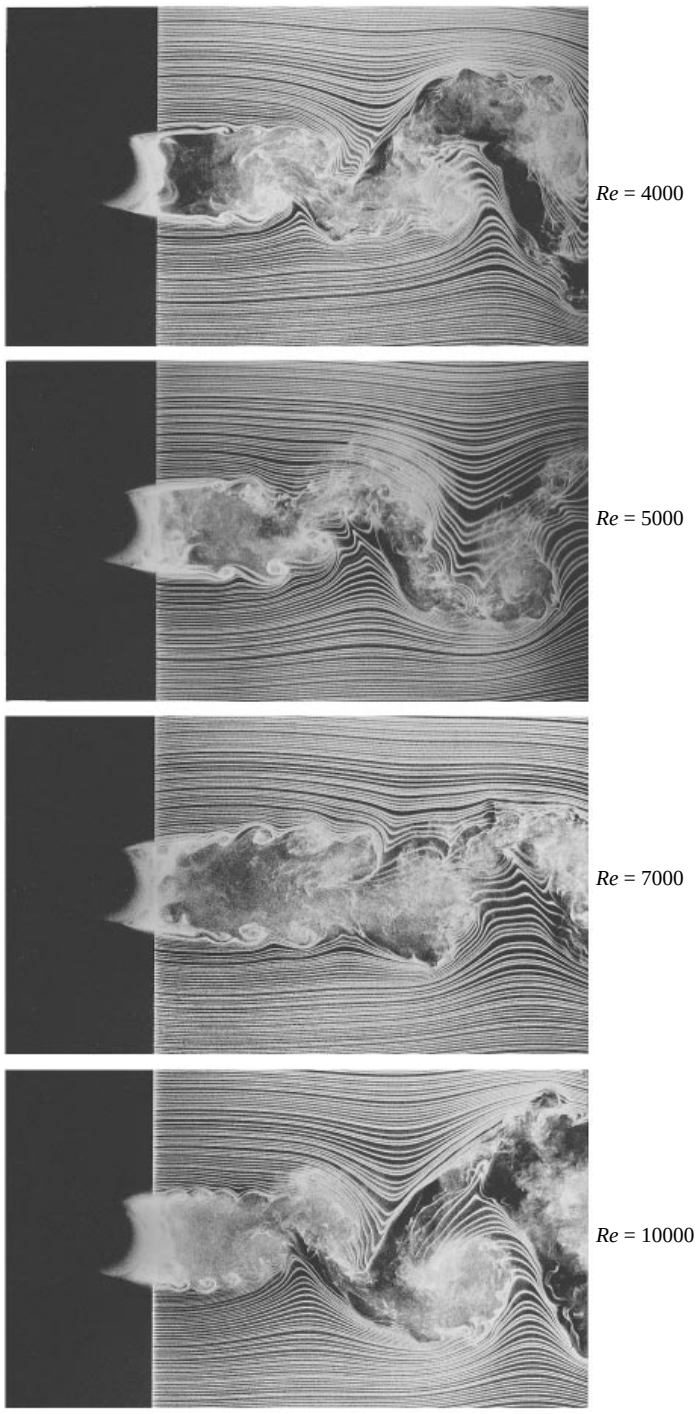

FIGURE 11. Cross-sectional view of the near wake at various Reynolds numbers. The shear-layer instability is observed to intensify as *Re* increases. It appears that the instability is in-phase across the wake, although this is not the only configuration which was recorded. The smoke wire is placed immediately downstream of the base of the cylinder (of diameter 2.54 cm), which was not fitted with endplates.

and small-amplitude shear-layer fluctuations is conceivably the result of a switching between these two modes, one of which has a larger growth rate than the other.

In summary, we find that the observed intermittency in shear-layer fluctuations is not caused by the transverse motion of the shear layer, but is principally the result of a random streamwise motion of the transition point, which is influenced by temporal changes in near-wake three-dimensional structures.

5. Frequency of shear-layer instability

Our investigation has, up to this point, addressed various aspects of velocity fluctuations in the shear layer. Finally, we would like to focus on the characteristic frequency of the shear-layer instability, f_{SL}. The shear-layer frequency may be evaluated from long-time-averaged velocity spectra, in which case f_{SL} is defined as the frequency corresponding to the maximum in the broad-band peak discussed with reference to figures 2 and 3. Regarding the measurement of shear-layer frequency, it is of interest to confirm that the spectral peak at f_{SL} does indeed correspond reasonably to predictions which can be made from measurements of τ_{SL} (period of shear-layer fluctuations) using time traces. (This question was raised by J. Mihailovic & T. Corke at the APS Meeting, 1995, private communication.) We have computed τ_{SL} directly from time traces, such as the one displayed in figure 6(*a*); however, since time traces indicate that the frequency is approximately constant within each packet, but may vary somewhat between packets, it becomes necessary to select a statistically significant sample to produce a reasonable value for τ_{SL}. To demonstrate that the two methods of determining shear-layer frequency are consistent, we have constructed a histogram (using over 200 shear-layer fluctuation cycles) shown in figure 12(*a*), where the frequency computed from each packet was weighted by the number of cycles in that packet. The frequency measured from long-time-averaged velocity spectra, shown by the arrowhead, is found to agree remarkably well with the most prominent bin in the histogram, which shows a consistency between the two techniques of measurement. However, since the technique using time traces is considerably more laborious, all of our subsequent measurements of shear-layer frequency are made from velocity spectra.

Before proceeding with our measurements of the normalized shear-layer frequency, we would like to highlight variations (of f_{SL}/f_K vs. Re) obtained by previous investigators. To determine these variations, we have independently analysed the actual data points from each investigation, utilizing an accurate digitizing tablet to extract frequency data from relevant plots of previous investigations. Our own analysis of these data, shown in table 1, indicates that the exponent, denoted p, in the expression

$$\frac{f_{SL}}{f_K} = A \times Re^{\,p},$$

is clearly larger than 0.5 in every case. In addition, there is a fair amount of scatter in the value of the exponent, which prompted us to make our own independent measurements of f_{SL}/f_K. Noting that in many of the previous studies end conditions were not well-defined, we have intentionally imposed parallel shedding conditions on the cylinder for our measurements.

In figure 12(*b*), we show the variation of normalized shear-layer frequency with Re, including only data from the present study and from Norberg (1987). These two sets of data show clearly that a power law can sufficiently describe this variation, at least over the range $10^3 < Re < 50 \times 10^3$, in this particular figure. The large symbol

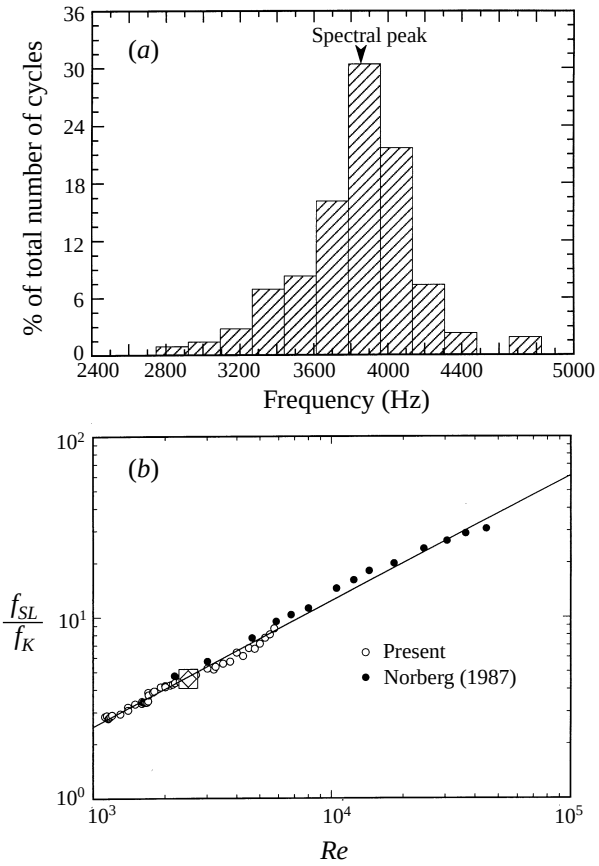

FIGURE 12. The measurement of shear-layer frequency from time traces at $Re = 2500$ compares very well with spectral measurements, as shown in the histogram in (*a*). The histogram is constructed from a sample of over 200 shear-layer fluctuation cycles. The arrow marker is the value of f_{SL} evaluated from long-time-averaged velocity spectra. In (*b*) is shown the variation of normalized shear-layer frequency with Re, using data from the present study and from Norberg (1987). The least-squares best-fit curve through these data (shown by the solid line) is $f_{SL}/f_K = 0.0207 \times Re^{0.69}$. The large symbol, calculated from the mean value of the histogram in (*a*), is found to agree well with the spectral measurements. The measurements are made at $x/D = 1.0$ and $y/D \approx 0.8$.

at $Re = 2500$ is calculated using the mean value from the histogram in figure 12(*a*). As mentioned above, it agrees well with the spectral data. A power law of the form $f_{SL}/f_K = 0.0207 \times Re^{0.69}$ fits both of these sets of data in a least-squares best-fit sense.

We now include all the available normalized shear-layer frequency data and arrive at the variation displayed in figure 13. The solid line, which is the least-squares best-fit line through all of these data concatenated, has the form

$$\frac{f_{SL}}{f_K} = 0.0235 \times Re^{0.67}\,. \tag{5.1}$$

It is clear that a power law of the form $Re^{0.5}$, shown as the broken line in figure 13, will not adequately represent the variation of normalized shear-layer frequency. This is particularly evident if one looks along the lines, with one's nose close to the frequency axis. In table 1 is included the power-law fit from our data alone, and that from (5.1). Equation (5.1) is reasonably unaffected by the presence of oblique

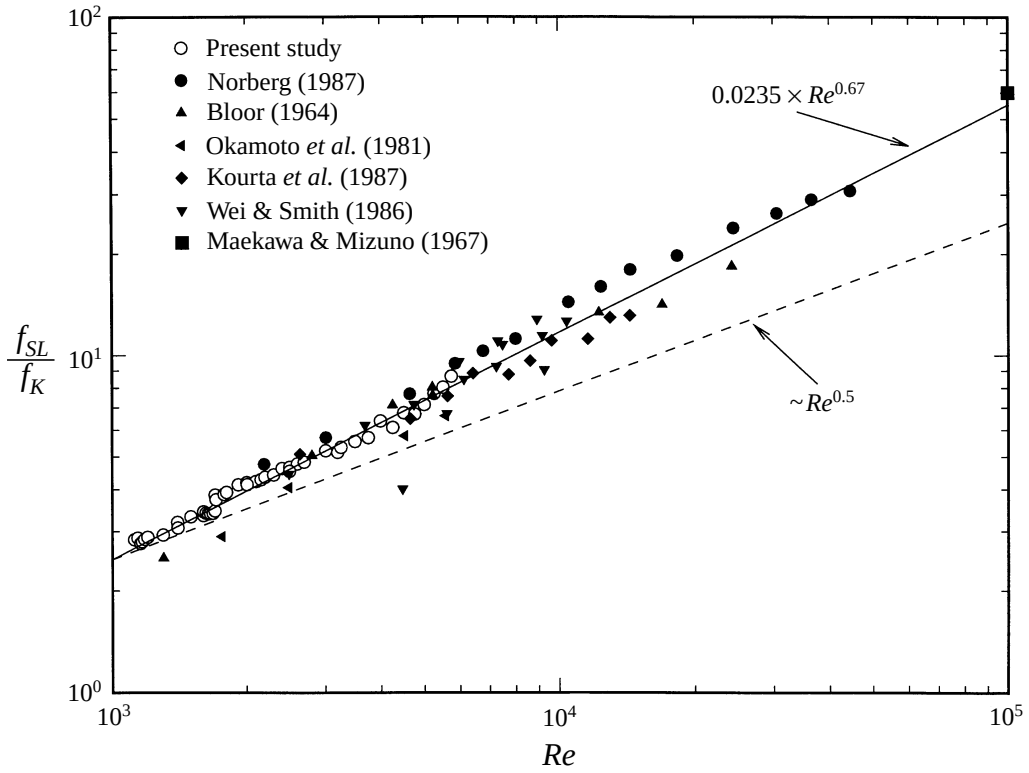

FIGURE 13. Variation of normalized shear-layer frequency with Reynolds number. The plot includes data from all the investigators who have measured the shear-layer frequency. The least-squares best-fit curve through all of these data is $f_{SL}/f_K = 0.0235 \times Re^{0.67}$. A curve of the form $Re^{0.5}$ is included as the broken line, for comparison. The isolated data point of Maekawa & Mizuno (1967) at $Re = 10^5$ lends some support for an $Re^{0.67}$ variation to be valid for $Re > 50 \times 10^3$. The present measurements are made at $x/D = 1.0$ and $y/D \approx 0.8$.

or parallel shedding, yielding an estimated variation in the exponent of around 0.01 if there was a mix of oblique and parallel shedding over this range of Re. Although the power law in (5.1) applies over the range of Re up to 50×10^3, it cannot be said whether or not a power law would be a good fit over the entire regime up to $Re = 2 \times 10^5$ (the boundary-layer transition critical Reynolds number), without further detailed measurements. However, it is necessary to draw attention to an isolated data point from the work of Maekawa & Mizuno (1967) who found that $f_{SL}/f_K = 60$ at $Re = 10^5$. Interestingly, the corresponding value computed from our least-squares best-fit power law (5.1), is $f_{SL}/f_K = 55$. As a comparison, we have used the $Re^{1/2}$-variation suggested by Kourta *et al.* (1987), to compute $f_{SL}/f_K = 30$ at $Re = 10^5$, which is significantly lower than the experimentally measured value. It therefore appears that there is some evidence which supports the power law (5.1) to be reasonably valid for Re up to 10^5.

In case it may be construed that the reasonably large number of data points in the present study weights the exponent of the concatenated data close to our own exponent, we would like to indicate that if one determines the least-squares best-fit exponent from all of the other data (excluding ours), one arrives at a variation of the form $Re^{0.7}$. If, in fact, the data of Wei & Smith (with the highest exponent) is

Investigation	Coefficient, A	Exponent, p	Re-range
Bloor (1964)	0.0277	0.6509	1300–25 000
Okamoto, Hirose & Adachi (1981)	0.0170	0.6925	1700–5600
Wei & Smith (1986)	0.0078	0.7997	2500–11 000
Kourta *et al.* (1987)	0.0507	0.5811	2600–15 000
Norberg (1987)	0.0346	0.6444	2200–44 500
Present study	0.0269	0.6587	1200–6000
All of the above data	0.0235	0.6742	1200–44 500

TABLE 1. A comparison of power-law variations from various studies. The data for normalized shear-layer frequency from each investigation have been fitted to an equation of the form $f_{SL}/f_K = A \times Re^p$. The range of Re from each of these studies is comparable.

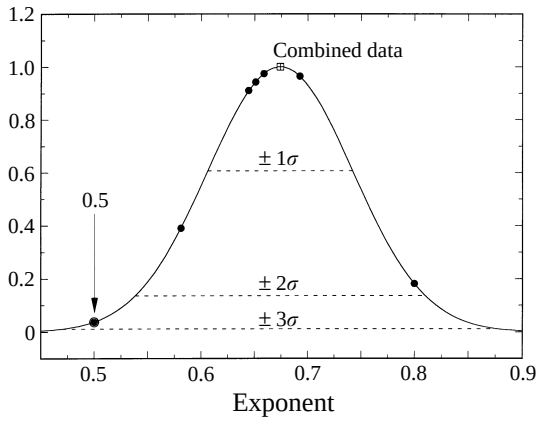

FIGURE 14. Visual display of the exponents from different investigations. The exponents have been determined by independently re-analysing the actual data from each investigation. The symbol σ represents one standard deviation of exponents listed in table 1, from the least-squares best-fit exponent. The hitherto extensively used exponent, 0.5, is found to lie nearly 3σ from the least-squares best-fit exponent of (5.1).

discounted, the average of all the other exponents (not all the data points) results in an exponent of 0.64, which is still significantly larger than 0.5. To further clarify this point, we present in figure 14 the exponents from all the studies overlaid on a Gaussian distribution, with the least-squares best-fit exponent from (5.1) placed at its apex. The standard deviation of the exponents in table 1 from the exponent of (5.1), has been indicated as σ in figure 14. We observe, immediately, that the exponent 0.5 lies nearly three standard deviations away from this least-squares best-fit exponent. Therefore, one can conclude quite definitively that the true exponent for the Re-variation of the normalized shear-layer frequency, is significantly larger than the hitherto extensively used value 0.5.

6. Physical considerations to explain the $Re^{0.67}$ power law

We present, here, a discussion which suggests why one should actually expect the exponent to be greater than 0.5. On a dimensional basis, it is to be expected that the shear-layer frequency will scale with a characteristic velocity and with a length scale

of the form

$$f_{SL} \sim \frac{U_{sep}}{\theta_t}, \tag{6.1}$$

where U_{sep} is the velocity outside the boundary layer at the separation point and θ_t is the momentum thickness of the separated shear layer at the 'transition point'. The 'transition point', defined by Sato (1956) for the case of a laminar separated shear layer, refers to the location at which the shear layer develops an instability, discernible as sinusoidal velocity fluctuations. By transition point, we do not mean the location of transition-to-turbulence which occurs further downstream. Sato (1956) determined the transition point from measurements of normalized turbulence energy integrated across the width of the shear layer. He suggested that transition occurs at the point at which this energy begins to increase rapidly. Furthermore, Sato (1956) found that the transition point, as defined above, varies linearly with the momentum thickness at the separation point (θ_{sep}), in the form

$$s_t \approx 47\ \theta_{sep}, \tag{6.2}$$

where s_t is the distance from the point of separation to the transition point, measured along the shear layer.

At $Re = 2000$, using the relationship $(U_{sep}/U_\infty) = (1 - C_{P_B})^{1/2}$ and the base suction coefficient from figure 7(*b*), we calculate a velocity of $1.35\,U_\infty$ outside the boundary layer at the separation point. At the same Re and at $x/D = 1.0$, we measure a velocity on the outer side of the shear layer of $1.27\,U_\infty$, from the profile in figure 1. This pair of calculations was repeated for $Re = 2600$, $Re = 4500$ and $Re = 5400$, from which it was found that the velocity on the outer side of the shear layer is only 6% lower at $x/D = 1.0$ than it is at the point of separation. Therefore, it appears that this velocity remains virtually constant over a streamwise distance of the order of one diameter, and our choice of velocity scale will be taken as U_{sep}. It should be noted that this choice of velocity scale is matched more closely as Reynolds number is increased, since the point of transition moves upstream with increasing Reynolds number as we indicate below. Regarding the precise value of length scale which should govern the shear-layer frequency, there seem to be several reasonable choices available in the literature. Experimenters who have studied the unforced plane mixing layer (see the review by Ho & Huerre 1984) appear to have used the value of momentum thickness at the origin of the mixing layer, and although this is a reasonable scale, it would not be suitable for the present problem. In this work, we wish to explicitly account for the upstream motion of the region of instability with Re (Linke 1931) and we assume that the characteristic length scale is one which also moves upstream as Re increases. Unal & Rockwell (1984, 1988*a*) suggested a characteristic momentum thickness, upon which the frequency is found to scale, measured at the middle of the linear growth region of shear-layer instability in the cylinder wake. We suggest, from a physical viewpoint, that the characteristic length scale which governs the frequency should be the momentum thickness (θ_t) in the vicinity of the location at which perturbations grows to perceptible proportions.

The scaling in (6.1), when used in conjunction with the definition of the Strouhal number, $S = f_K D/U_\infty$, yields

$$\frac{f_{SL}}{f_K} \sim \frac{1}{S}\left(\frac{U_{sep}}{U_\infty}\right)\left(\frac{D}{\theta_t}\right). \tag{6.3}$$

In order to predict the Re-variation of f_{SL}/f_K, it is necessary to determine how

each term on the right-hand side of (6.3) varies. We begin with the development of the momentum thickness (θ) of the shear layer. Bloor (1964) suggested that the normalized momentum thickness at the separation point scales with $Re^{-1/2}$ such that

$$\frac{\theta_{sep}}{D} = \frac{A}{Re^{1/2}}, \tag{6.4}$$

where A is a constant. Immediately following separation, and at least up to the transition point, the separated shear layer develops like a laminar mixing layer and spreads as $(s + s_o)^{1/2}$ (Sato 1956), where s is the distance measured along the shear layer from the point of separation and $(-s_o)$ is the location of the virtual origin of the shear layer, which we assume to be constant here but justify presently. The streamwise variation of the momentum thickness can, therefore, be represented in the form

$$\frac{\theta}{D} = B\left(\frac{s}{D} + \frac{s_o}{D}\right)^{1/2}. \tag{6.5}$$

The parameter B can be found in terms of A, using conditions at the separation point (where $s = 0$), and the development of the momentum thickness takes the form

$$\frac{\theta}{D} = \frac{A}{Re^{1/2}}\left(\frac{s/D}{s_o/D} + 1\right)^{1/2}. \tag{6.6}$$

From (6.6) it is now possible to determine the momentum thickness θ_t at the transition point s_t, and this when substituted into (6.3) yields

$$\frac{f_{SL}}{f_K} \sim \frac{Re^{1/2}}{S}\frac{U_{sep}}{U_\infty}\left(\frac{s_t/D}{s_o/D} + 1\right)^{-1/2}. \tag{6.7}$$

Now, if one assumes that the shear-layer frequency does not depend on the position of transition, implying that the term in parentheses in (6.7) is constant, and that U_{sep}/U_∞ and S are approximately constant, then the variation suggested by Bloor (1964) is recovered,

$$\frac{f_{SL}}{f_K} \sim Re^{1/2}. \tag{6.8}$$

Despite the fact that such assumptions appear very reasonable, they are only approximately correct over a large range of Re. If we use the result that $(U_{sep}/U_\infty) = (1 - C_{P_B})^{1/2}$ in (6.7), we find

$$\frac{f_{SL}}{f_K} \sim Re^{1/2}\frac{(1 - C_{P_B})^{1/2}}{S}\left(\frac{s_t/D}{s_o/D} + 1\right)^{-1/2}. \tag{6.9}$$

The base suction coefficient increases with Reynolds number, for $Re > 1200$, as shown by the meticulous work of Norberg (1994). Therefore, we expect the ratio U_{sep}/U_∞ to increase over a large range of Re. Moreover, S decreases, albeit slowly, over the Re-range under consideration. Consequently, one expects the value of the exponent to be greater than 0.5. Furthermore, the position of transition in the shear layers moves upstream with increasing Re, shown by Linke (1931) and Schiller & Linke (1933), and is equivalent to s_t/D decreasing as Re increases. Thus the most unstable frequency is larger than if the frequency were dictated by conditions at a fixed downstream location in the shear layer.

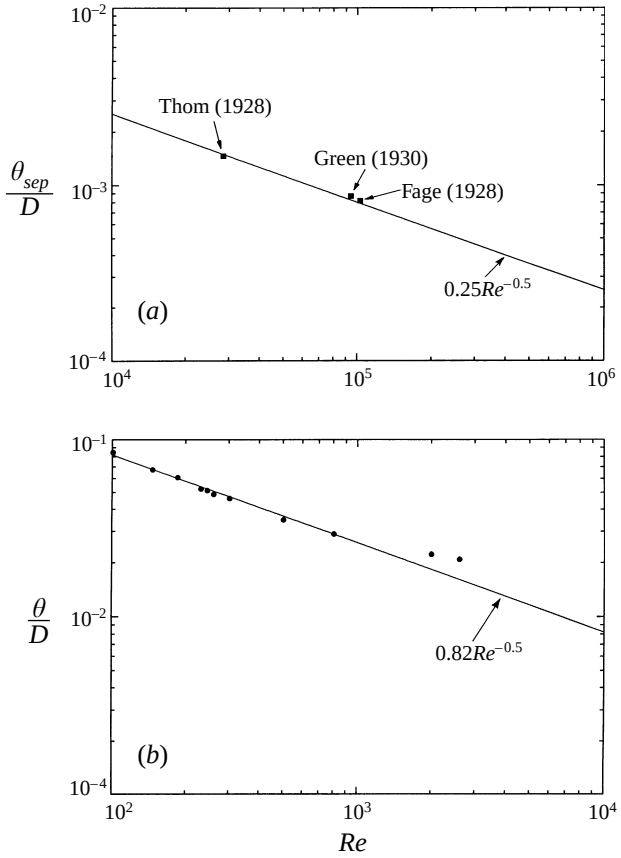

FIGURE 15. Variation of the shear-layer momentum thickness with Re. The momentum thickness at the point of separation, in (a), has been determined from the boundary-layer velocity profile measurements of Thom (1928), Fage (1928) and Green (1930). The measurements of the momentum thickness at $x/D = 1.0$, in (b), are from Williamson (1997). It is found that both momentum thicknesses are well-represented by an $Re^{-1/2}$ variation.

Using (6.4) in (6.2), we find the variation

$$\frac{s_t}{D} = 47\,\frac{A}{Re^{1/2}}\,. \tag{6.10}$$

Substituting (6.10) into (6.9), produces the following variation for the normalized shear-layer frequency:

$$\frac{f_{SL}}{f_K} \sim \frac{(1-C_{P_B})^{1/2}}{S}\,\frac{Re^{1/2}}{(CRe^{-1/2}+1)^{1/2}}\,, \tag{6.11}$$

where $C = 47\,A\,(D/s_o)$. To predict the Re-variation of f_{SL}/f_K from (6.11), it is necessary to determine the constant C. We have determined $A = 0.25$, as shown in figure 15(a), by evaluating the momentum thickness at the point of separation from the boundary-layer velocity profile measurements of Thom (1928), Green (1930) and Fage (1928). Williamson (1997) found that the momentum thickness of the shear layer varies as $0.82\,Re^{-1/2}$, at a distance of one diameter downstream of the axis of the cylinder, as shown in figure 15(b). This result was utilized in (6.6) to determine

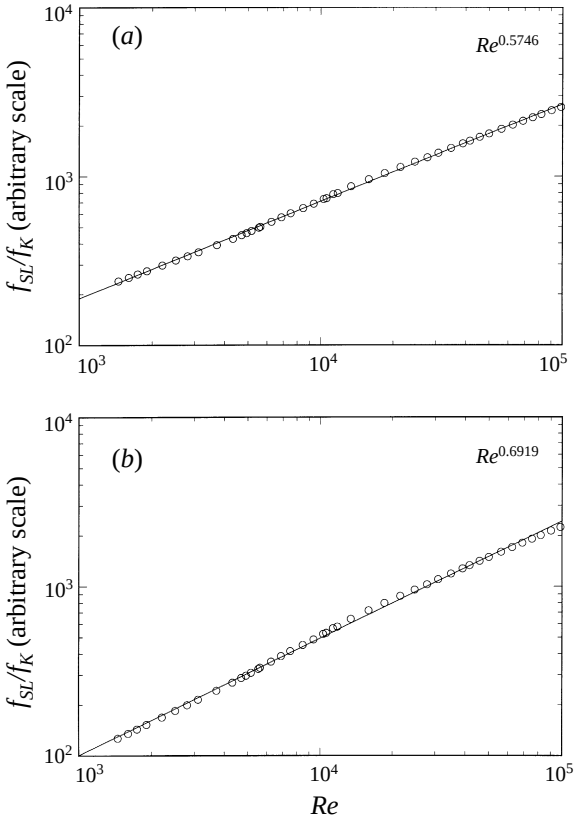

FIGURE 16. Predicted shear-layer frequency using the data of Norberg (1987). In (*a*) is shown the variation predicted by ignoring the effect of upstream motion of the transition point. However, accounting for this upstream motion, and using (6.11) produces the variation shown in (*b*). In each case, the least-squares best-fit power-law variations are indicated; the vertical axes are only proportional to f_{SL}/f_K.

$s_o/D = 0.12$. We have calculated $s_o/D \approx 0.12$ at $Re = 28 \times 10^3$ from the measurements of Thom (1928) and $s_o/D \approx 0.13$ at $Re = 100 \times 10^3$ from the work of Fage (1928), from which it appears that s_o/D is virtually constant over a range which spans almost one decade in Reynolds number, and justifies our earlier assumption of constant s_o/D. Therefore, the constant $C \approx 100$, and the term $C\,Re^{-1/2}$ is never much larger than unity for the Re-range in which the shear-layer instability manifests itself, implying that the second term in the denominator of the second term in (6.11) cannot be neglected compared to the first.

Using measured values of $(-C_{P_B})$ and S over a large range of Re, from Norberg (1994), it is now possible to predict the variation of the shear-layer frequency from (6.11). We have found that the predicted variation of f_{SL}/f_K with Re is well-represented by a power law. If, to first order, we neglect the entire denominator of the second term in (6.11), we arrive at the variation shown in figure 16(*a*), for which the least-squares best-fit line is of the form $f_{SL}/f_K \sim Re^{0.57}$. This is the power-law variation of f_{SL}/f_K when one accounts only for the variations in U_{sep} (or $-C_{P_B}$) and S, as Reynolds number is varied.

If we now include the denominator of the second term, which accounts for the upstream motion of the transition point with Re as well, we find the variation shown

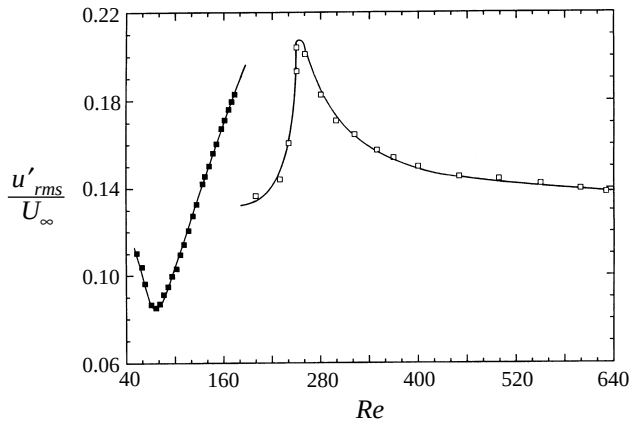

FIGURE 17. The apparent 'resonance' in $(u'_{rms}/U_\infty)_{Total}$ at $Re = 260$. The power-law variation from (5.1), when extrapolated to lower Re, seems to indicate that the shear-layer frequency would be equal to the vortex-shedding frequency at $Re = 262$, thereby suggesting a wake–shear-layer interaction which produces a 'resonance' in wake characteristic parameters at this Re. The solid symbols are data from Williamson (1996*b*) and the open ones from Prasad & Williamson (1997). The measurements are made at $x/D = 10.0$ and $y/D \approx 1.0$.

in figure 16(*b*), for which the least-squares best-fit line is of the form

$$\frac{f_{SL}}{f_K} \sim Re^{0.69}. \tag{6.12}$$

The above simple analysis, based on physical arguments, appears to produce an exponent for the Re-variation of the normalized shear-layer frequency which is in good agreement with that obtained from experimental measurements.

One might wonder if the predicted shear-layer frequency using (6.11) is sensitive to the precise value of C. We show, below, that the predicted variation in (6.12) is remarkably robust to changes in the value of $C = 47\,A\,(D/s_o)$, where the parameter 47 is obtained from the work of Sato (1956). As mentioned above, s_o/D is found to be virtually invariant with Re. The constant A was also similarly evaluated and found to vary by less than 7% among the three studies. Since the parameter from the work of Sato (1956) depends on the level of free-stream turbulence, one may expect it to produce a reasonable variation in the value of C. To intentionally over-estimate the change in exponent due to alterations in C, we assume that C varies by 50% due to variations in its constituents. We find that even a 50% change in C produces a variation in the exponent of only 0.025. The predicted variation of f_{SL}/f_K therefore seems to be robust to variations in the precise value of C.

7. Discussion

Despite the fact that the shear-layer instability is observed only for $Re > 1200$, one could question whether the instability would influence wake parameters at lower Reynolds numbers. Such a question arises because of the occurrence of a remarkable maximum in wake characteristic parameters found in the three-dimensional transition regime ($190 < Re < 260$), as described in the following. Williamson & Roshko (1990) and Norberg (1994) found a local maximum in $(-C_{P_B})$ at $Re \approx 260$. Furthermore, Prasad & Williamson (1997) have found that the total fluctuation intensity, $(u'_{rms}/U_\infty)_{Total}$, shown in figure 17, rises very rapidly through the three-dimensional

transition regime and attains a remarkable peak at $Re \approx 260$, with a similar peak also occurring for $(u'_{rms}/U_\infty)_{f_K}$. From flow visualization, Williamson (1996*b*) and Prasad & Williamson (1997) have found that the primary vortex shedding which is particularly spanwise-coherent at $Re \approx 260$ is reminiscent of the shedding observed in the laminar regime, with the exception of a superimposed fine-scale three-dimensionality. In addition, time traces show that velocity fluctuations appear to be particularly periodic at $Re \approx 260$, producing a distinctly sharp peak at f_K in long-time-averaged velocity spectra. All of these observations are suggestive of some sort of a 'resonance' in wake characteristic parameters at $Re \approx 260$. An attempt to understand why this resonance occurs, led us to examine (5.1) more closely. By a simple manipulation, (5.1) can be recast into a more appropriate form,

$$\frac{f_{SL}}{f_K} = \left(\frac{Re}{262}\right)^{0.67}, \tag{7.1}$$

from which it is immediately deduced that $f_{SL}/f_K = 1$ when $Re = 262$. The fact that the observed resonance in wake parameters occurs at a Reynolds number when $f_{SL}/f_K = 1$ from the above equation, may perhaps be a coincidence. Alternatively, one may suggest that this resonance is due to an interaction between the wake and the shear layer, when the primary wake frequency would be equal to the shear-layer frequency. Although a convincing proof of this interaction is still lacking, further details are presented in Williamson (1996*b*).

8. Conclusions

In the present investigation, we have found that the spanwise end conditions which control the primary vortex shedding from the cylinder significantly affect the instability of the separated shear layer. By imposing parallel shedding conditions, the inception of instability occurs at $Re_c \approx 1200$; however, the use of oblique shedding conditions inhibits the development of instability until $Re_c \approx 2600$. The dependence of the critical Reynolds number on the spanwise end conditions, in the absence of the effects of a variation in free-stream turbulence, could explain much of the enormous scatter found in quoted values of Re_c. Despite the fact that the angle of primary vortex shedding affects the inception of shear-layer instability, we find that it does not influence the orientation of the shear-layer instability, since flow visualizations demonstrate that the shear-layer instability is inherently two-dimensional, irrespective of the particular mode of primary vortex shedding.

We confirm the existence of intermittency in shear-layer fluctuations, as found previously in the theses of Norberg (1987) and Cardell (1993). We demonstrate that the intermittent nature of the shear-layer fluctuations is not associated with the transverse motion of the shear layers past a stationary probe, as has been previously suggested. We find that the random (streamwise) motion of the point of transition is principally responsible for the intermittency in shear-layer fluctuations measured at a fixed point. One may expect that this streamwise movement of the transition point is influenced by the temporal changes in the near-wake three-dimensionality, in the form of Mode B streamwise vortices. Periods of upstream movement of the transition point, and the most vigorous presence of shear-layer instability, seem to coincide when there exists an in-phase synchronization of the shear-layer vortices in a 'varicose' configuration.

With respect to the shear-layer frequency, we find, from a complete re-examination

of data from previous investigators, that a power-law of the form $Re^{1/2}$ does not accurately represent the variation of f_{SL}/f_K. In fact, a consideration of all the data from previous studies, including our own measurements, results in the variation

$$\frac{f_{SL}}{f_K} = 0.0235 \times Re^{0.67}.$$

The above equation appears to be valid for Re up to 10^5. We present an argument, based on simple physical ideas, which suggests why one would naturally expect an exponent larger than 0.5. The analysis takes account of the Re-variation of the velocity and length scales that govern the shear-layer frequency, which are influenced by the variations in the base pressure, Strouhal number and the upstream motion of the transition point, as Reynolds number is increased, resulting in the relationship

$$\frac{f_{SL}}{f_K} \sim Re^{0.7},$$

which is in a good agreement with the direct experimental measurements.

Finally, despite the fact that the shear-layer instability is not manifested for $Re <$ 1200 from hot-wire measurements, it appears that the observed 'resonance' in wake characteristic parameters at $Re \approx 260$ is possibly caused by an interaction between the wake and the shear layer, when f_{SL}/f_K would be equal to unity.

The authors would like to express their gratitude to Thomas Leweke for several stimulating discussions and enthusiastic assistance during paper preparation. This work has been supported by the ONR Grant Nos. N-00014-94-1-1197 and N-00014-95-1-0332.

REFERENCES

Bloor, M. S. 1964 The transition to turbulence in the wake of a circular cylinder. *J. Fluid Mech.* **19**, 290.

Braza, M., Chassaing, P. & Ha Minh, H. 1990 Prediction of large-scale transition features in the wake of a circular cylinder. *Phys. Fluids* A **2**, 1461.

Cardell, G. S. 1993 Flow past a circular cylinder with a permeable wake splitter plate. PhD thesis, Graduate Aeronautical Laboratory, California Institute of Technology.

Corke, T., Koga, D., Drubka, R. & Nagib, H. 1977 A new techinique for introducing controlled sheets of streaklines in wind tunnels. *IEEE Publication* 77-CH 1251-8 AES.

Fage, A. 1928 The air flow around a circular cylinder in the region where the boundary layer separates from the surface. *British Aero. Res. Council R&M* 1179.

Gerrard, J. H. 1978 The wakes of cylindrical bluff bodies at low Reynolds number. *Phil. Trans. R. Soc. Lond.* A **288**, 351.

Green, J. J. 1930 The viscous layer associated with a circular cylinder. *British Aero. Res. Council R&M* 1313.

Ho, C.-M. & Huerre, P. 1984 Perturbed free shear layers. *Ann. Rev. Fluid Mech.* **16**, 365.

Kourta, A., Boisson, H. C., Chassaing, P. & Ha Minh, H. 1987 Nonlinear interaction and the transition to turbulence in the wake of a circular cylinder. *J. Fluid Mech.* **181**, 141.

Lin, J.-C., Vorobieff, P. & Rockwell, D. 1996 Space-time imaging of a turbulent near-wake by high-image-density particle image cinematography. *Phys. Fluids* **8**, 555.

Linke, W. 1931 Neue Messungen zur Aerodynamik des Zylinders, insbesondere seines reinen Reibungswiderstandes. *Phys. Zr.* **32**, 900.

Maekawa, T. & Mizuno, S. 1967 Flow around the separation point and in the near-wake of a circular cylinder. *Phys. Fluids Suppl.* S184.

Norberg, C. 1987 Effect of Reynolds number and a low-intensity freestream turbulence on the flow around a circular cylinder. *Publ.* 87/2. Dept. Applied Thermodynamics and Fluid Mechanics, Chalmers University of Technology.

Norberg, C. 1994 An experimental investigation of the flow around a circular cylinder: influence of aspect ratio. *J. Fluid Mech.* **258**, 287.

Okamoto, S., Hirose, T. & Adachi, T. 1981 The effect of sound on the vortex-shedding from a circular cylinder. *Bull. JSME* **24**, 45.

Peterka, J. A. & Richardson, P. D. 1969 Effects of sound on separated flows. *J. Fluid Mech.* **37**, 265.

Prasad, A. & Williamson, C. H. K. 1995 Three-dimensional effects in turbulent bluff body wakes. In *Proc. Tenth Symp. Turbulent Shear Flows.* Pennsylvania State University.

Prasad, A. & Williamson, C. H. K. 1996 The instability of the separated shear layer from a bluff body. *Phys. Fluids* **8**, 1347.

Prasad, A. & Williamson, C. H. K. 1997 Three-dimensional effects in turbulent bluff body wakes. Submitted to *J. Fluid Mech.*

Roshko, A. 1954 On the drag and shedding frequency of two-dimensional bluff bodies. *NACA TN* 3169.

Roshko, A. 1993 Perspectives on bluff body aerodynamics. *J. Wind Ind. Aerodyn.* **49**, 79.

Sato, H. 1956 Experimental investigation on the transition of laminar separated layer. *J. Phys. Soc. Japan* **11**, 702.

Schiller, L. & Linke, W. 1933 Pressure and frictional resistance of a cylinder at Reynolds numbers 5000 to 40 000. *NACA TM* 715.

Smith, R. A., Moon, W. T. & Kao, T. W. 1972 Experiments on flow about a yawed circular cylinder. *Trans. ASME J. Basic Engng* **94**, 771.

Thom, A. 1928 The boundary layer of the front portion of a cylinder. *British Aero. Res. Council R&M* 1176.

Unal, M. F. & Rockwell, D. 1984 The role of shear layer stability in vortex shedding from cylinders. *Phys. Fluids* **27**, 2598.

Unal, M. F. & Rockwell, D. 1988*a* On vortex shedding from a cylinder. Part 1. The initial instability. *J. Fluid Mech.* **190**, 491.

Unal, M. F. & Rockwell, D. 1988*b* On vortex shedding from a cylinder. Part 2. Control by splitter-plate interference. *J. Fluid Mech.* **190**, 513.

Wei, T. & Smith, C. R. 1986 Secondary vortices in the wake of circular cylinders. *J. Fluid Mech.* **169**, 513.

Williamson, C. H. K. 1988 The existence of two stages in the transition to three-dimensionality of a cylinder wake. *Phys. Fluids* **31**, 3165.

Williamson, C. H. K. 1996*a* Vortex dynamics in the cylinder wake. *Ann. Rev. Fluid Mech.* **28**, 477.

Williamson, C. H. K. 1996*b* Three-dimensional wake transition. *J. Fluid Mech.* **328**, 345.

Williamson, C. H. K. 1997 Wake formation behind a bluff body. In preparation for *J. Fluid Mech.*

Williamson, C. H. K. & Roshko, A. 1990 Measurement of base pressure in the wake of a cylinder at low Reynolds numbers. *Z. Flugwiss. Weltraumforsch.* **14**, 38.

Wu, J., Sheridan, J., Hourigan, K. & Soria, J. 1996 Shear layer vortices and longitudinal vortices in the near wake of a circular cylinder. *Exp. Thermal Fluid Sci.* **12**, 169.